Nuclear Science and Techniques **22** (2011) 217–223

Directly radiolabeled phage with spleen-targeting specificity

SUN Liyan LIANG Kun[#] WANG Xiangyun CHU Taiwei[*]

Beijing National Laboratory for Molecular Sciences, *Radiochemistry and Radiation Chemistry Key Laboratory of Fundamental Science*, *College of Chemistry and Molecular Engineering*, *Peking University*, *Beijing 100871*, *China*

Abstract Phage display technique is a powerful approach for discovering new tumor- and organ-targeting ligands, and radiolabeled phage has a potential to analyze the phage-binding sensitivity and specific imaging. In this study, phage II (the spleen-targeting phage) in mice was isolated after three rounds biopanning, and labeled by ^{99m}Tc using mercaptoacetyltriglycine (MAG_3) as chelator to evaluate their binding properties *in vivo*. The amount of phage II eluted from spleen was enriched by plague assay each round. ^{99m}Tc-MAG_3-phage II showed the less retention in blood at any time point than half that of ^{99m}Tc-MAG_3-phage I (the radiolabeled original Ph.D-12 phage as control). The accumulation in spleen between ^{99m}Tc-MAG_3-phage I and II was of different tendency. The highest uptake of ^{99m}Tc-MAG_3-phage II in spleen was 24.80 %ID/g at 30 min; and of ^{99m}Tc-MAG_3-phage I, 30.93% ID/g at 5 min. After circulating ^{99m}Tc-MAG_3-phage II for 120 min, its accumulation in spleen decreased though higher than that of ^{99m}Tc-MAG_3-phage I. In other organs, the ^{99m}Tc-MAG_3-phage II showed low retention and high spleen-to-organ or tissue ratios. In conclusion, the radiolabeled phage II is convenient for studying the binding and specificity of spleen-targeting peptides found via phage display *in vivo*.

Key words Radiolabeling, Phage display, Spleen-targeting, Reticuloendothelial system, Biodistribution

1 Introduction

Spleen, an important lymphoreticular organ, is capable of filtering infectious microorganisms, particles and macromolecules from the blood. Developing effective splenotropic agent is a crucial task in experimental and clinical medicine. As a novel passive targeting approach in splenotropic drug delivery[1], particles coated with poloxamer and poloxamine block co-polymers consisting of polyethylene oxide and poly-propylene oxide can be delivered to the spleen[2,3]. The particles modified by the amphiphilic copolymer [poly methoxy poly(ethylene glycol) cyanoacrylate-co-hexadecyl cyanoacrylate] (PEG-PHDCA) has a higher splenic uptake than the non-modified nano- particles after a long circulation time *in vivo*[4]. The unique vascular structure and target site in the spleen[5] need novel ligands enhancing splenic uptake in spleen-otropic drug delivery[1].

Having such advantages as rapid screening process, easy operation, low cost, and easy identification of diversity of peptides, phage display technique with high-throughput screen is widely used to study protein-protein, protein-peptide, and protein-DNA interactions. Since 1985[6], thousands of tumor- and organ-targeting peptides have been isolated by the technique[7]. Geier *et al.*[8] found that the spleen contained the highest phage titer with a retention time of up to 7 days, and the result was echoed by Molenaar *et al.*[9], indicating that uptake of ^{35}S-labeled M13 phage was predominated by reticuloendothelial system (RES). The large phage accumulating in spleen is difficult for phage display to identify its specificity *in vivo*, and no direct evidence shows that the uptake of phage in spleen is non-specific.

Supported by National Natural Science Foundation of China (No. 20771011 and 21071010) and the Ministry of Science and Technology of China (No. 2006CB705700)

# SUN L Y and LIANG K contributed equally to this work.

* Corresponding author. *E-mail address*: twchu@pku.edu.cn

Received date: 2011-01-25

The binding properties of phage to its target can be quantified. An *E. coli* infecting is traditional plaque immunoassay, such as ELISA (enzyme-linked immuno sorbent assay), which reduces the effect of elution efficiency[10,11]. The fluorochrome labeling[12, 13] can help to visualize the binding location. Also radiolabeled phage with ^{32}P[14] , ^{35}S[11], ^{111}In[15], and ^{99m}Tc[16,17] are potential agents for infection diagnosis and specific imaging due to rapid and economical labeling, high stability in saline and serum, uniform viability and infectivity to host bacteria [18].

In this work, spleen-targeting phage II was identified by an *in vivo* phage display, and labeled with ^{99m}Tc. The biodistribution of ^{99m}Tc-MAG_3-phage II in normal mice was examined.

2 Materials and methods

2.1 Reagents and equipments

All reagents were of analytical grade and used without further purification. Phage I (the Ph.D-12 phage display peptide library kit) was purchased from NEB (New England Biolabs, Beijing, China). Bacto-tryptone, yeast extract, PEG (polyethylene glycol with average M = 8 000), DMEM (Dulbecco's Modified Eagle Medium) and agar were from Beijing Xinjingke Biotechnology Co. (China). PEG/NaCl and LB medium (a mixture of 10 g bacto-tryptone, 5 g yeast extract, 5 g NaCl, and in 1 L distilled water) were prepared according to procedures of the NEB product manual. DMEM-P1 is a mixture containing the protease inhibitor (phenylmethylsulphonyl fluoride, 1 mM), aprotinin (20 μg/mL) and leupeptin (1 μg/mL) in DMEM). NHS-MAG_3 (N-hydroxysuccinimidyl S-acetylmercapto-acetyltriglycinate) was synthesized in our laboratory.

The ^{99m}Tc-pertechnetate was eluted from a ^{99}Mo-^{99m}Tc generator (China Institute of Atom Energy, Beijing). The radioactivity of tissue samples were analyzed by a gamma counter (Packard, USA), and radioactivity of ^{99m}Tc-labeled products were determined by a FT-630 γ well counter (Beijing Nuclear Instrument Factory, China).

Kunming mice (20–22g, male) were purchased from the Breeding Center of Zoology at Peking University Health Science Center, China. All experiments were carried out in accordance with the principles of laboratory animal care and regulations for the administration of affairs concerning experimental animals in China.

2.2 Phage selection

Biopanning procedures were carried out according to the NEB product manual and methods reported previously[19–21]. About 10^{11} PFU of the randomized phage I suspended in PBS was injected into the mice tail vein. After 5 min, the mice were killed by cervical dislocation. The spleens were quickly removed. They were washed with ice-cold water, homogenized in the ice-cold DMEM-P1 (1 mL), and washed two times with ice-cold DMEM-P1. The phage bound to spleen was recovered by incubation of 1 mL bacterial culture solution (*Escherichia coli* 2738) at room temperature for 30 min. After titrating, amplifying and purifying, the phage was injected into mice as described above. The isolated phage after three rounds of biopanning was collected as phage II.

2.3 Conjugation of phage with MAG_3 chelator

Conjugation procedures were performed according to Refs.[16] and [17]. Briefly, sodium bicarbonate of 2–4 μL (0.1 M, pH 9.0) was mixed with PBS of 200 μL containing about 10^{10} PFU/mL phage I or II. The fresh NHS-MAG_3 solution (1 g/L, DMF) of 4 μL was added under stirring at room temperature for 45 min. After adding the PEG/NaCl solution of 35 μL, the mixture was incubated on ice for over 15 min, and the PEG precipitate was centrifuged for 15–20 min at 10000 rpm/min at 4ºC. Again, the MAG_3-phage I or II was suspended in PBS and precipitated by PEG/NaCl. Finally, MAG_3-phage I or II was suspended in PBS and stored at 4ºC.

2.4 MAG_3-phage radiolabeled with ^{99m}Tc[16,17]

^{99m}Tc-pertechnetate generator eluant (3.7×10^7 Bq), 20 μL sodium tartrate (30 mg/mL), and 2 μL fresh $SnCl_2\cdot2H_2O$ solution (1 mg/mL in 0.01 M HCl) were added into 100 μL MAG_3-phage I or II (10^{10} PFU/mL). The mixture was incubated at room temperature for 30 –60 min, and purified by precipitation twice with PEG /NaCl. The ^{99m}Tc-MAG_3-phage I or II was suspended in PBS. The radiochemical purity was estimated by

paper chromatography (Whatman No.1, VWR, Boston, MA) using saline as solvent, and cut strips of 1 cm were used to determine radioactivity by the gamma well counter.

2.5 Stability of ^{99m}Tc-MAG$_3$-phage in PBS

Stability of the ^{99m}Tc-MAG$_3$-phage I or II was evaluated by paper chromatography using saline as solvent. The ^{99m}Tc-MAG$_3$-phage I or II (100 μL, 10^{11} PFU) in 0.4-mL PBS at 37ºC was taken in duplicate for 1 and 3 h.

2.6 Biodistribution of ^{99m}Tc-MAG$_3$-phage in mice

The ^{99m}Tc-MAG$_3$-phage I or II (100 μL, about 10^9 PFU/mL, 8.6×10^5 Bq) was injected via tail vein injection to the mice (five mice per group). After circulating for 5, 30, 60 and 120 min, the mice were killed by cervical dislocation. The blood samples were drawn from the eye orbit. The organs or tissues such as spleen, heart, brain and liver were removed, washed and weighed prior to radioactivity counting. The 100-μL injection solution as a standard was used to calculate the injected dose per gram in tissue (%ID/g), and the ratio of spleen to organ or tissue per mouse was expressed as the mean±SD. The ^{99m}Tc-MAG$_3$-phage I was used as negative control.

3 Results

3.1 *In vivo* screening for spleen-targeting phage

The Ph.D-12 peptide phage library (phage I) was used to screen spleen-specific phage. After three rounds of selecting, the eluted phage was enriched from spleen as shown by the plaque assay data in Table 1, and the recovery ratios of 10^{-7}–10^{-6} were in accord with Ref. [22]. The round 3 recovery ratio was three times higher than round 1; and twice than round 2. The amplified and purified phage of the last round was collected as phage II (the spleen-specific phage), and recovery ratio was obtained by the PFU of the eluate over the input PFU.

3.2 Radiochemical purity of ^{99m}Tc-MAG$_3$-phage

The radiochemical purity of ^{99m}Tc-MAG$_3$-phage II was over 90% as indicated by the paper chromatography results (Fig.1c). The ^{99m}Tc-MAG$_3$-phage II in paper/saline system remained at the origin (R_f=0.0), whereas ^{99m}Tc-MAG$_3$ (R_f =0.9), ^{99m}Tc-tartrate (R_f =0.6), and ^{99m}Tc-pertechnetate (R_f = 0.8) migrated at different flow rates (Figs.1d, 1e, and 1f). The radiochemical purity of ^{99m}Tc-MAG$_3$-phage I was the same as that of ^{99m}Tc- MAG$_3$-phage II.

Table 1 Results of panning rounds of phage I in spleen.

Panning rounds	Total input PFU	Total eluate PFU	Recovery (eluate/input)
1	2.8×10^{12}	9.7×10^5	3.5×10^{-7}
2	4.2×10^{12}	2.3×10^6	5.4×10^{-7}
3	2.5×10^{12}	2.7×10^6	1.1×10^{-6}

3.3 Stability of ^{99m}Tc-MAG$_3$-phage in buffer

Fig.2 shows the percent activity of ^{99m}Tc-MAG$_3$-phage I and II by strip chromatography in PBS over 60 and 180 min. The radioactivity of ^{99m}Tc-MAG$_3$-phage I and II remained 85–90% after incubation for 180 min. This is consistent with Ref.[16], and indicates that the radiolabeled phage is stable under the incubation conditions, especially in serum.

3.4 Clearance of ^{99m}Tc-MAG$_3$-phage in the blood

The biodistribution of ^{99m}Tc-MAG$_3$-phage II were close to those of ^{99m}Tc-MAG$_3$-phage I, with similar clearance time from the blood but different relative accumulation. In Fig.3A, more than 8 %ID/g uptake of ^{99m}Tc-MAG$_3$-phage I and about 4 %ID/g uptake of ^{99m}Tc-MAG$_3$-phage II were in the blood at 5 min, indicating that ^{9m}Tc-MAG$_3$-phage II accumulated in the spleen resulted in low retention in the blood.

3.5 Biodistribution of ^{99m}Tc-MAG$_3$-phage in mice

The biodistribution results of ^{99m}Tc-MAG$_3$-phage II in normal mice at different time points are shown in Figs. (3) and (4). The liver and spleen uptakes were the highest, and in accord with our previous report [17]. The uptake in liver at 5 min was 31.4 %ID/g for ^{99m}Tc-MAG$_3$-phage II and 44.08 %ID/g for ^{99m}Tc- MAG$_3$-phage I, and went down with time (Fig.3B). However, the highest ^{99m}Tc-MAG$_3$-phage II uptake in spleen was 24.80 %ID/g at 30 min; and the ^{99m}Tc-MAG$_3$-phage I, 30.93% ID/g at 5 min (Fig.3C). After circulating for 120 min, the ^{99m}Tc-MAG$_3$-phage II accumulation in spleen decreased, but was still higher than that of ^{99m}Tc-MAG$_3$-phage I, indicating that ^{99m}Tc-MAG$_3$-

phage II was cleared more slowly than ^{99m}Tc-MAG$_3$-phage I, and likely to bind to some special sites.

Fig.3D shows the uptake of the ^{99m}Tc-MAG$_3$-phage II in bone was 0.7 %ID/g–1.0 %ID/g from 30 to 120 min. The uptake of ^{99m}Tc-MAG$_3$-phage I rose quickly after 30 min, up to 4.63 %ID/g, which is three times higher than that of ^{99m}Tc-MAG$_3$-phage II. It was 0.95 %ID/g at 120 min, indicating that the bone-targeting phage was largely cleared after three rounds selection and the capture of phage particles by reticuloendothelial system (RES) was not totally non-specific but selective.

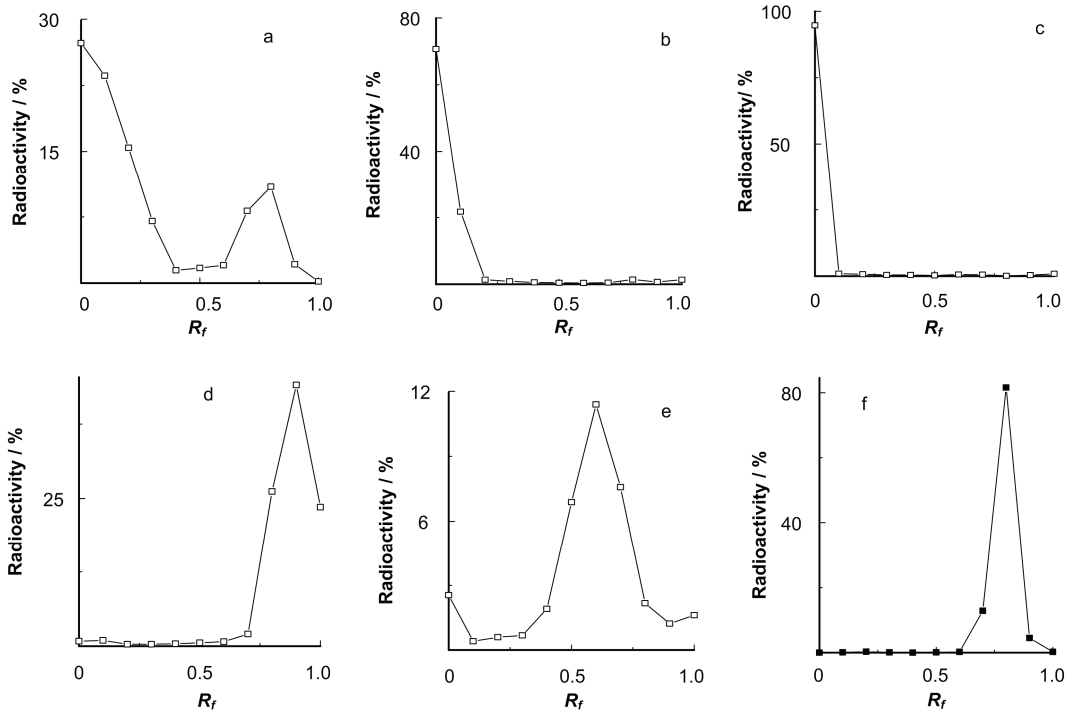

Fig.1 Paper chromatograms of ^{99m}Tc-MAG$_3$-phage II. Before purification (a), After one (b) and two (c) purification procedures; ^{99m}Tc-MAG$_3$ (d), ^{99m}Tc-tartrate (e) ^{99m}Tc-pertechnetate (f) in paper/saline system.

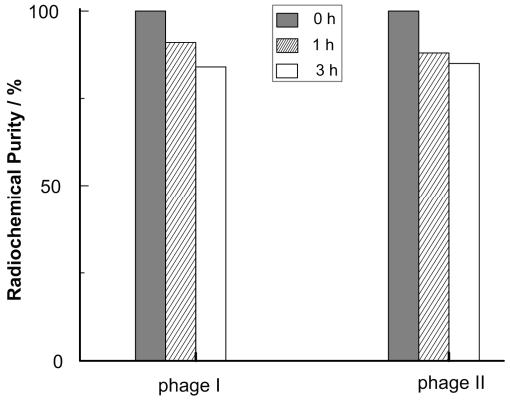

Fig.2 Stability of ^{99m}Tc-MAG$_3$-phage I and II in PBS.

Also, Fig.4B shows that ^{99m}Tc-MAG$_3$-phage II has low retention in other tissues and organs. Prior to 120 min, there was little ^{99m}Tc-MAG$_3$-phage II in brain (0.03%ID/g). The uptake in heart, pancreas and muscle was low (0.45%ID/g, 0.35%ID/g, and 0.22%ID/g, respectively). The radioactivity in digestive system increased slightly with time, from 0.91%ID/g to 2.23%ID/g in intestine and from 1.71%ID/g to 3.62%ID/g in stomach. The increased uptake in stomach and intestine would be related to the metabolism of ^{99m}Tc-MAG$_3$-phage II in mice. The uptake of ^{99m}Tc-MAG$_3$-phage II in non-target organ was mainly less than that of ^{99m}Tc-MAG$_3$-phage I, which contributed to increased homing of phage II in spleen.

4 Discussion

Panning *in vivo* represents a significantly new application in phage display technique[6,20,21], improving the correlation between the binding of phage and their targeting molecule. Using this methodology, a number of novel peptides reacting with organ-specific endothelium and parenchyma makers had been selected [22–32].

We investigated phage II targeting spleen by phage display *in vivo*. The biodistribution of ^{99m}Tc-

MAG_3-phage II was evaluated in normal mice at different time points. Control experiment was performed to determine the non-specific uptake of ^{99m}Tc-MAG_3-phage I.

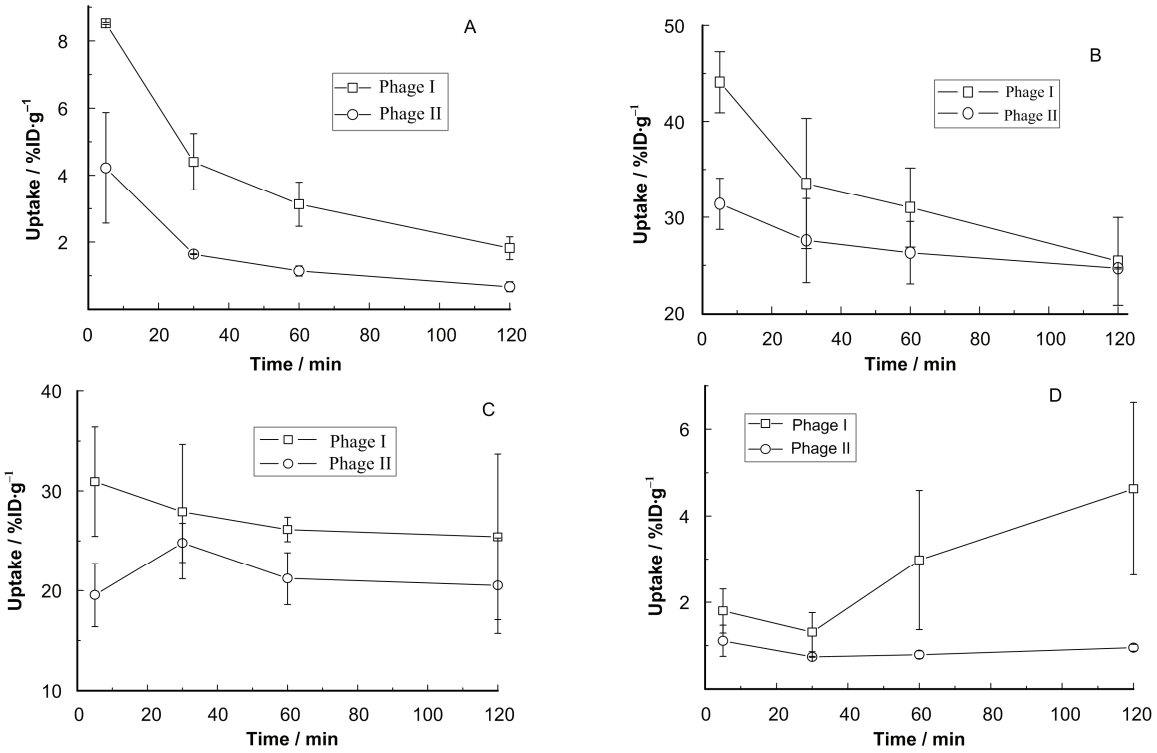

Fig.3 Biodistribution of ^{99m}Tc- 99mTc-MAG3-phages in mice in the blood (A), liver (B), spleen(C), and bone (D).

Fig.4 shows the uptake of ^{99m}Tc-MAG_3-phage II in organs from 5 to 120 min. The retention in liver and spleen is the highest, and the least in muscle, pancreas, and brain, but the retention in spleen did not increase significantly after three rounds panning. However, the radioactivity peak of ^{99m}Tc-MAG_3-phage II in spleen appeared at 30 min and lasted longer than that of ^{99m}Tc-MAG_3-phage I, indicating that ^{99m}Tc-MAG_3-phage II had a longer retention than ^{99m}Tc-MAG_3-phage I in spleen. The uptake (%ID/g) of ^{99m}Tc -MAG_3-phage I in spleen decreased with time, and the uptake (%ID/g) of ^{99m}Tc-MAG_3-phage II in spleen remained constant (Fig.3C). This suggests that retention of phage II in spleen might be related to the selective binding. Comparatively, the uptakes of ^{99m}Tc -MAG_3-phage I and II in the liver are similar (Fig.3B), indicating that the highest accumulation in liver mainly resulted from phagocytosis by the mononuclear phagocytic system (MPS) cells in liver[8,9,16,33–37]. However, except for phagocytosis, there is another mechanism of particle clearance by the spleen[38,39], indicating a unique target sites consisting of cell and vascular structure, cell growth factor, and protein receptor.

Table 2 shows spleen/organ or spleen/tissue ratios for ^{99m}Tc-MAG_3-phages I and II at various time points. All spleen/blood ratios for ^{99m}Tc-MAG_3-phage II were higher than that for ^{99m}Tc-MAG_3-phage I, and increased to 33.69 after 120 min, while it was 12.55 for ^{99m}Tc-MAG_3-phage I. The spleen/liver ratio for ^{99m}Tc-MAG_3-phages II was around 0.8 after 30 min, which is close to the data of ^{99m}Tc-MAG_3-phage I. Significant increases in spleen/intestine (33.07 for large intestine, 44.93 for small intestine), spleen/ muscle (75.88), spleen/brain (361.14) and spleen/bone (33.51) were obtained by circulating ^{99m}Tc-MAG_3-phage II in mice after 30 min. Most of them are higher than ^{99m}Tc-MAG_3-phage I (19.77, 23.6, 32.39, 165.86, 21.29, respectively). The spleen/brain ratio for ^{99m}Tc-MAG_3-phage II quickly went up to 783.77, while it is 313.39 for ^{99m}Tc-MAG_3-phage I at 120 min. The spleen/bone ratio of ^{99m}Tc-MAG_3-phage II rose up to 33.51 after 30 min and dropped slowly to 24.75 after 120 min, while the ratio of ^{99m}Tc-MAG_3-phage I fell to 3.69 after 120 min. The longer retention time and higher spleen-to-organ/tissue ratios of ^{99m}Tc- MAG_3-

phage II suggest that there may be no non- specific accumulation in spleen by the RES. The spleen-specific peptide ligands have opportunity to be obtained by phage display *in vivo*.

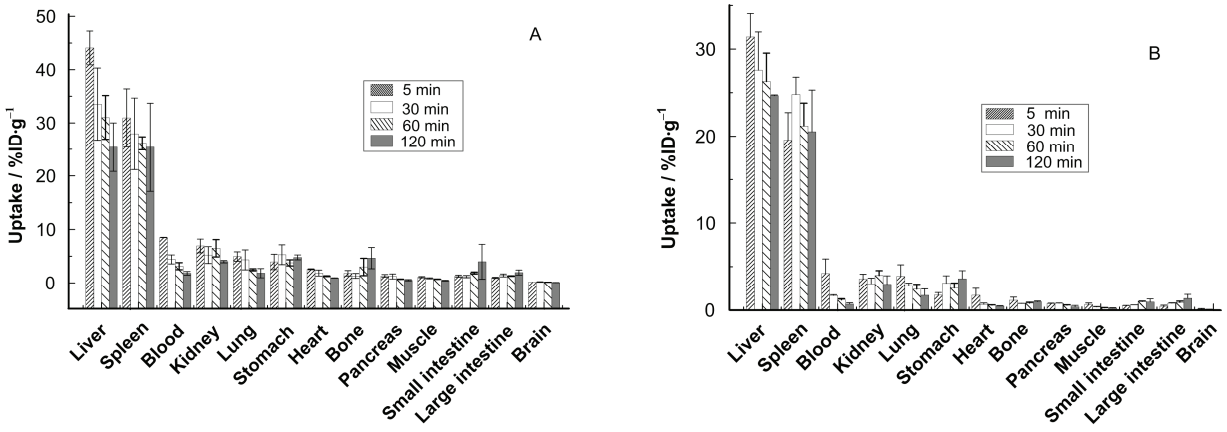

Fig.4 Tissue distribution of ^{99m}Tc-labeled phages in normal mice at 5, 30, 60, and 120 min after administration. (A) ^{99m}Tc-MAG_3-phage I and (B) ^{99m}Tc-MAG_3-phage II.

Table 2. The ratios of spleen to tissue after injection of ^{99m}Tc labeled phage.

Spleen/organs		Ratios			
		5 min	30 min	60 min	120 min
Spleen/liver	^{99m}Tc-MAG_3-Phage I	0.71±0.11	0.79±0.04	0.77±0.10	0.83±0.25
	^{99m}Tc-MAG_3-Phage II	0.65±0.12	0.89±0.21	0.81 ±0.09	0.83±0.11
spleen/heart	^{99m}Tc-MAG_3-Phage I	12.09±2.06	15.06±0.61	12.79±1.51	35.25±2.92
	^{99m}Tc-MAG_3-Phage II	10.21±1.09	40.44±7.35	41.67±3.71	55.57±4.31
Spleen/kidney	^{99m}Tc-MAG_3-Phage I	4.46±0.51	5.35±0.24	2.59±0.73	5.39±0.67
	^{99m}Tc-MAG_3-Phage II	5.86±0.21	8.06±2.13	5.62±0.85	6.76±0.74
spleen/lung	^{99m}Tc-MAG_3-Phage I	6.25±1.18	6.27±0.97	6.89±0.14	9.11±2.02
	^{99m}Tc-MAG_3-Phage II	4.67±2.24	9.12±3.07	9.61±2.62	12.78±1.98
Spleen/blood	^{99m}Tc-MAG_3-Phage I	3.63±0.59	6.35±1.99	5.21±0.61	12.55±3.35
	^{99m}Tc-MAG_3-Phage II	4.49±1.29	15.95±2.11	19.71±2.49	33.69±0.91
Spleen/stomach	^{99m}Tc-MAG_3-Phage I	7.86±2.55	5.28±2.38	4.34±0.43	4.48±0.21
	^{99m}Tc-MAG_3-Phage II	12.14±0.31	7.37±2.67	8.41±2.11	5.73±0.48
Spleen/Large intestine	^{99m}Tc-MAG_3-Phage I	31.75±7.23	19.77±3.77	12.80±0.47	12.45±3.13
	^{99m}Tc-MAG_3-Phage II	50.83±18.95	33.07±4.78	26.30±4.31	21.68±5.92
Spleen/Small intestine	^{99m}Tc-MAG_3-Phage I	24.20±3.67	23.66±1.15	8.79±1.48	9.97±4.56
	^{99m}Tc-MAG_3-Phage II	42.14±6.36	44.93±3.68	23.89±1.09	21.12±5.31
Spleen/pancreas	^{99m}Tc-MAG_3-Phage I	23.57±1.60	23.10±2.67	23.73±2.30	48.29±8.01
	^{99m}Tc-MAG_3-Phage II	28.77±2.67	34.40±4.08	40.36±5.12	65.71±13.23
Spleen/muscle	^{99m}Tc-MAG_3-Phage I	28.95±8.63	32.39±2.83	14.20±5.41	43.98±6.15
	^{99m}Tc-MAG_3-Phage II	33.33±5.67	75.88±9.20	90.13±5.26	106.86±8.36
Spleen/bone	^{99m}Tc-MAG_3-Phage I	17.17±3.88	21.29±1.67	5.65±2.11	3.69±2.51
	^{99m}Tc-MAG_3-Phage II	18.91±5.92	33.51±2.67	28.48±3.78	24.75±3.90
Spleen/brain	^{99m}Tc-MAG_3-Phage I	193.54±24.28	165.86±11.49	121.70±19.8	313.39±5.98
	^{99m}Tc-MAG_3-Phage II	210.43±11.49	361.14±45.97	562.02±55.29	783.77±48.05

On the other hand, the radiolabeled phage shows the evidence of evaluating binding specificity. Rusckowski *et al.*[16] demonstrated ^{99m}Tc-labeled M13 filamentous phage bound specifically to its bacterial host, *E.coli*, *in vitro* and *in vivo*. Other four ^{99m}Tc-labeled phages were applied in infection imaging[18].

Consistent with the detailed studies by biodistribution of phages in mice[9,34,36], we reasoned that ^{99m}Tc-labeled phage maintaining original characteristics, such as infectivity, metabolism, specific binding activity, could be developed as a convenient and fast tool to assess target affinity and selectivity *in vitro* and *in vivo*, especially in microSPECT imaging.

5 Conclusions

The RES-rich organs such as spleen were usually recognized to non-specifically retain phage particles, and the spleen-targeting phage was isolated and confirmed by phage display *in vivo*. Also, it is meaningful to investigate the specific spleen-targeting peptides by *in vivo* phage display technique in the near future.

Reference

1 Devarajan P V, Jindal A B, Patil R R, *et al*. J Pharm Sci, 2010, **99:** 2576–3581.

2 Moghimi S M, Hedeman H, Muir I S, *et al*. Biochim Biophys Acta, 1993, 1157: 233–240.

3 Moghim S M, Porter C J H, Muir I S, *et al*. Biochem Biophys Res Commun, 1991, **177:** 861–866.

4 Calvoa P, Gouritin B, Brigger I, *et al*. J Neurosci Meth, 2001, **111:** 151–155.

5 Moghimi S M. Adv Drug Delivery Rev, 1995, **17:** 103–115.

6 Smith G P. Science, 1985, **228:** 1315–1317.

7 Deutscher S L. Chem Rev, 2010, **110:** 3196–3211.

8 Geier M R, Trigg M E, Merril C R. Nat, 1973, **246:** 221–223.

9 Molenaar T J M, Michon I, de Haas S A M, *et al*. Virology, 2002, **293:** 182–191.

10 Naik R R, Jones S E, Murray C J, *et al*. Adv Funct Mater, 2004, **14:** 25–30.

11 Curtis S B, Hewitt J, MacGiliivray R T A, *et al*. Biotechnol Bioeng, 2009, **102:** 644–650.

12 Jaye D L, Geigerman C M, Fuller R E, *et al*. J Immunol Meth, 2004, **295:** 119–127.

13 Kelly K A, Waterman P, Weissleder R. Neoplasia, 2006, **8:** 1011–1018.

14 Carter D M, Radding C M. J Biol Chem, 1971, **216:** 2502–2512.

15 Newton J R, Miao Y B, Deutscher S L, *et al*. J Nucl Med, 2007, **48:** 429–436.

16 Rusckowski M, Gupta S, Liu G Z, *et al*. J Nucl Med, 2004, **45:** 1201–1208.

17 Sun L Y, Chu T W, Wang X Y, Prog Biochem Biophys, 2006, **33:** 1200–1206.

18 Rusckowski M, Gupta S, Liu G Z, *et al*. Nucl Med Biol, 2008, **35:** 433–440.

19 Arap W, Pasqualini R, Ruoslahti E. Sci, 1998, **279:** 377–380.

20 Pasqualini R, Ruoslahti E. Nat, 1996, **380:** 364–366.

21 Lee T Y, Wu H C, Tseng Y L, *et al*. Cancer Res, 2004, **64:** 8002–8008.

22 Rajotte D, Arap W, Hagedorn M, *et al*. J Clin Invest, 1998, **102:** 430–437.

23 Joyce J A, Laakkonen P, Bernasconi M, *et al*. Cancer Cell, 2003, **4:** 393–403.

24 Kolonin M G, Sun J, Do K A, *et al*. FASEB J, 2006, **20:** 979–981.

25 Kolonin M G, Bover L, Sun J, *et al*. Cancer Res, 2006, **66:** 34–40.

26 Kolonin M G, Saha P K, Chan L, *et al*. Nat Med, 2004, **10:** 625–632.

27 Arap M A, Lahdenranta J, Mintz P J, *et al*. Cancer Cell, 2004, **6:** 275–284.

28 Arap W, Kolonin M G, Trepel M, *et al*. Nat Med, 2002, **8:** 121–127.

29 Sato M, Arap W, Pasqualini R. Oncology, 2007, **21:** 1346–1352.

30 Ozawa M G, Zurita A J, Dias-Neto E, *et al*. Trends Cardiovas Med, 2008, **18:** 126–132.

31 Cardó-Vila M, Zurita A J, Giordano R J, *et al*. PLoS One, 2008, **3:** e3452.

32 Staquicini F I, Tandle A, Libutti S K, *et al*. Cancer Res, 2008, **68:** 8419–8428.

33 Pasqualini R, Koivunen E, Ruoslahti E. Nat Biotechnol, 1997, **15:** 542–546.

34 Zou J, Dickerson M T, Owen N K, *et al*. Mol Biol Reports, 2004, **31:** 121–129.

35 Inchley C J. Clin Exp Immunol, 1969, 5: 173–187.

36 Yip Y L, Hawkins N J, Smith G, *et al.* J Immunol Meth, 1999, **225:** 171–178.

37 Storm G, Belliot S O, Daemen T, *et al*. Adv Drug Deliv Rev, 1995, **17:** 31–48.

38 Smith L P, Hunter K W, Oldfeild E C, *et al.* Infec Immunity, 1982, **38:** 162–167.

39 Classen E, Van Rooijen N, Biochim. Biophys. Acta, 1984, **802:** 428–434.